
BAYESIAN CONDITIONAL AUTO-REGRESSIVE LASSO MODELS TO LEARN SPARSE BIOLOGICAL NETWORKS WITH PREDICTORS

Yunyi Shen

Department of Statistics
University of Wisconsin-Madison
Madison, WI 53706

Claudia Solís-Lemus*

Wisconsin Institute for Discovery
University of Wisconsin-Madison
Madison, WI 53706

ABSTRACT

Microbiome data analyses require statistical models that can simultaneously decode microbes' reaction to the environment and interactions among microbes. While a multiresponse linear regression model seems like a straight-forward solution, we argue that treating it as a graphical model is flawed given that the regression coefficient matrix does not encode the conditional dependence structure between response and predictor nodes because it does not represent the adjacency matrix. This observation is especially important in biological settings when we have prior knowledge on the edges from specific experimental interventions that can only be properly encoded under a conditional dependence model. Here, we propose a chain graph model with two sets of nodes (predictors and responses) whose solution yields a graph with edges that indeed represent conditional dependence and thus, agrees with the experimenter's intuition on average behavior of nodes under treatment. The solution to our model is sparse via Bayesian LASSO and is also guaranteed to be the sparse solution to a Conditional Auto-Regressive (CAR) model. In addition, we propose an adaptive extension so that different shrinkage can be applied to different edges to incorporate edge-specific prior knowledge. Our model is computationally inexpensive through an efficient Gibbs sampling algorithm and can account for binary, counting and compositional responses via appropriate hierarchical structure. Finally, we apply our model to a human gut and a soil microbial composition datasets.

Keywords Linear Regression · Compositional Data · Interaction Network · Graphical model

1 Introduction

Recent years have seen explosion of microbiome research studies. Microbial communities are among the main driving forces of all biogeochemical processes on Earth. On one side, many critical soil processes such as mineral weathering, and soil cycling of mineral-sorbed organic matter are governed by mineral-associated microbes [13, 37, 8, 21, 38]. On another side, plant and soil microbiome drive phenotype variation related to plant health and crop production [2, 33, 24, 23]. In addition, as evidenced by The Human Microbiome Project [34], the microbes that live on the human body are key determinants of human health and disease [11].

Understanding the composition of microbial communities and what environmental or experimental factors play a role in shaping this composition is crucial to comprehend biological processes in humans, soil and plants alike, and to predict microbial responses to environmental changes. However, the inter-connectivity of microbes-environment is still not fully understood. One of the reasons for this gap in knowledge is the lack of statistical tools to infer connections among microbial communities while simultaneously accounting for predictors in a unified framework.

On the surface, the solution to this problem in linear regression settings seems straight-forward. On one side, (bayesian) graphical LASSO [14, 36] allows us to determine a sparse graphical model representation among responses via estimation of the sparse covariance matrix albeit without the inclusion of predictors. On the other side, a multiresponse linear regression model allows us to include multiple responses and predictors with LASSO techniques for sparse predictor solution. This could potentially be treated as a graphical model. Intuitively, the combination of these methods would provide a framework where researchers could estimate a sparse graphical structure with nodes for responses and for predictors.

*Corresponding author: solislemus@wisc.edu

We argue, however, that treating a multiresponse linear regression model as a graphical model is flawed and it should be done with caution. In particular, care should be taken to distinguish between marginal effects and conditional effects. This distinction is crucial when we would like to include biological prior knowledge to the model (e.g. as in [28]). For instance, penicillin has no biological effect on Gram-positive bacteria, yet it might still promote the abundance of such bacteria by inhibiting their Gram-negative competitors. In this example, penicillin has no *conditional* effect on Gram-positive nodes (conditioned on all other microbes), but it may have a *marginal* effect on them when marginalizing over all other microbes (Fig. 1 B). The inverse is also possible. A response can be conditionally dependent on a predictor, but marginally independent when another response has a similar dependence with that predictor (Fig. 1 F). In this case, the different link between the responses could marginally cancel out the effect of the predictor.

Here, we introduce a novel model framework to infer a complex network structure that represents both interactions among nodes and effects of a set of predictors. Specifically, our model estimates a network that represents the conditional dependence structure of a multivariate response (e.g. abundances of microbes) while simultaneously estimating the conditional effect of a set of predictors that influence the network (e.g. diet, weather, experimental treatments). Our model is represented by a chain graph [26, 25] with two sets of nodes: predictors and responses (Fig. 1). Directed edges between a predictor and a response represent conditional links, and undirected edges among responses represent correlations.

In addition to providing a more sensible representation compared to standard multiresponse linear regression, our model guarantees a sparse solution via Bayesian LASSO. As we will show later, the sparse solution of this model is guaranteed to also be the sparse solution of the Conditional Auto-Regressive (CAR) model [35]. This model is defined by full conditional distributions which assume a certain response is linear to predictors and other responses. To account for different prior knowledge, we also propose an adaptive extension that allows different shrinkage to different edges. Furthermore, we use our Normal model as a core and build hierarchical structures upon it to account for binary, counting and compositional responses. Finally, our model is able to equally handle small and big data and is computationally inexpensive through an efficient Gibbs sampling algorithm.

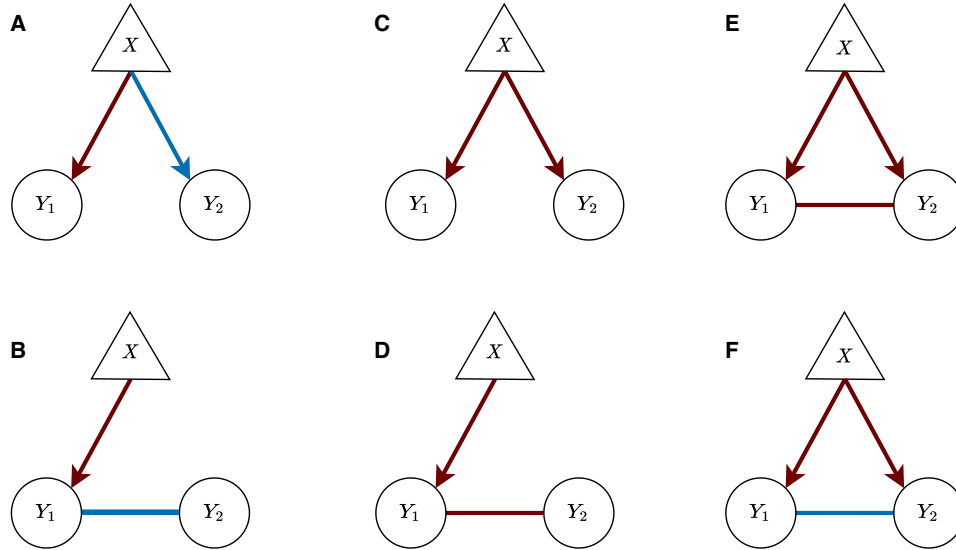


Figure 1: **Simple network with predictors.** We use a triangle to represent a predictor X and circles to represent the responses Y_1 and Y_2 . Red edges correspond to positive links between nodes while blue edges correspond to a negative links. Networks A and B (likewise networks C and D) can produce a similar marginal correlation structure between any two nodes. Distinguishing edges in E can be difficult since all edges have the same direction. Finally, in network F, X and Y_2 are conditionally correlated, yet they might not have a marginal correlation. For example, if Y_1, Y_2 had marginal variance 1 and covariance $\rho = -0.5$, while conditional regression coefficient between Y_1 and X conditioned on Y_2 was $\beta_1 = 2 > 0$ and conditional regression coefficient between Y_2 and X conditioned on Y_1 was $\beta_2 = 1 > 0$, we can show that the marginal regression coefficient between Y_2 and X when integrating out Y_1 is $\rho\beta_1 + \beta_2 = 0$ (more in Section 2.2).

2 Materials and methods

2.1 Model specification

Let $\mathbf{Y}_i \in \mathbb{R}^k$ be a multivariate response with k entries for $i = 1, \dots, n$ observations. Let $\mathbf{X}_i \in \mathbb{R}^{1 \times p}$ be the row vector of predictors for $i = 1, \dots, n$ (i.e. the i^{th} row of the design matrix $X \in \mathbb{R}^{n \times p}$). We assume that the design matrix is standardized so that each column has a mean of 0 and same standard deviation (set to be 1 in the simulations).

Let \mathbf{Y}_i follow a Normal distribution with mean vector $\Omega^{-1}(\mathbf{B}^T \mathbf{X}_i^T + \mu)$ and precision matrix $\Omega \in \mathbb{R}^{k \times k}$ (positive definite) where $\mathbf{B} \in \mathbb{R}^{p \times k}$ corresponds to the regression coefficients connecting the responses ($\mathbf{Y}_i \in \mathbb{R}^k$) and the predictors ($\mathbf{X}_i \in \mathbb{R}^{1 \times p}$) scaled by the marginal variance and $\mu \in \mathbb{R}^k$ corresponds to the intercept. We use the transpose $\mathbf{B}^T \mathbf{X}_i^T \in \mathbb{R}^{k \times 1}$ because samples are encoded as row vectors in the design matrix while by convention multivariate Normal samples are column vectors.

The likelihood function of the model is:

$$p(\mathbf{Y}_i | \mathbf{X}_i, \mu, \mathbf{B}, \Omega) \propto \exp[(\mathbf{B}^T \mathbf{X}_i^T + \mu)^T \mathbf{Y}_i - \frac{1}{2} \mathbf{Y}_i^T \Omega \mathbf{Y}_i]. \quad (1)$$

Note that in this parametrization, \mathbf{B} encodes *conditional dependence* between \mathbf{Y} and \mathbf{X} because in the kernel of the density, B_{ij} is the coefficient of product between X_i and Y_j . Thus, if $B_{ij} = 0$, then X_i and Y_j are *conditionally independent*. This is analogous to the case of Ω whose off-diagonal entries encode the conditional dependence between responses Y_i and Y_j .

From a graphical perspective, \mathbf{B} represents the adjacency matrix between response nodes (\mathbf{Y}) and predictor nodes (\mathbf{X}) while the off-diagonal entries of Ω represent the partial correlations which coincide with the adjacency matrix between response nodes. The yielding parameter estimations are indeed a adjacency matrix of a chain graph [3, 26, 15]

Correspondence to classical CAR. The parameters in the proposed model corresponds to a scale transformation of the classical conditional auto-regressive (CAR) model [35], and both models share sparse solutions. We can re-parametrize our model to the classical CAR parametrization as follows. Let \mathbf{B}' denote the unscaled conditional regression coefficients between responses and predictors. Let \mathbf{C} denote the conditional regression coefficients between responses, and let \mathbf{M} denote the conditional variance. We can generate the three matrices by decomposing Ω . Define diagonal matrix \mathbf{D} by $D_{ii} = \Omega_{ii}$ and $\mathbf{R} = \mathbf{D} - \Omega$. Then we can calculate $\mathbf{C} = \mathbf{D}^{-1} \mathbf{R}$, $\mathbf{M} = \mathbf{D}^{-1}$ and $\mathbf{B}' = \mathbf{D}^{-1} \mathbf{B}$ [35]. Though a sparse precision matrix (Ω) guarantees a sparse conditional auto-regression coefficient (\mathbf{C}), one needs to be careful about the negative sign in this transformation. Conditional auto-regression coefficients (\mathbf{C}) has an opposite sign as those in the precision matrix (Ω).

Prior specification. We assume a Laplacian prior on the entries of \mathbf{B} and graphical lasso prior on Ω [32, 36]. Using the Normal scale mixture representation of Laplace distribution [32, 36, 4], let η_{ml} be the latent scale parameters for Ω for $1 \leq m < l \leq k$ since Ω is symmetric and let τ_{ij} ($1 \leq i \leq p, 1 \leq j \leq k$) be the latent scale parameters for \mathbf{B} .

The full model specification is then:

$$\begin{aligned} \mathbf{Y}_i | \mathbf{X}_i, \mu, \mathbf{B}, \Omega &\sim N(\Omega^{-1}(\mathbf{B}^T \mathbf{X}_i^T + \mu), \Omega^{-1}) \\ B_{ij} | \tau_{ij} &\sim N(0, \tau_{ij}^2) \\ \tau_{ij} &\sim \frac{\lambda_\beta^2}{2} e^{-\lambda_\beta^2 \tau_{ij}} \\ p(\Omega | \eta, \lambda_\Omega) &= C_\eta^{-1} \prod_{m < l} \left[\frac{1}{\sqrt{2\pi\eta_{ml}}} \exp\left(-\frac{\omega_{ml}^2}{2\eta_{ml}}\right) \right] \prod_{m=1}^k \left[\frac{\lambda_\Omega}{2} \exp\left(-\frac{\lambda_\Omega \omega_{mm}}{2}\right) \right] I_{\Omega \in M^+} \\ p(\eta | \lambda_\Omega) &\propto C_\eta \prod_{m < l} \frac{\lambda_\Omega^2}{2} \exp\left(-\frac{\lambda_\Omega^2 \eta_{ml}}{2}\right) \end{aligned} \quad (2)$$

where $I_{\Omega \in M^+}$ means that Ω must be positive definite.

2.2 On conditional (in)dependence

In regression models for multivariate response, the regression coefficients linking a given response with the predictors can be conditional (conditioned on the other responses) or marginal (integrating out the other responses). In our model, the regression coefficients matrix \mathbf{B} encode conditional dependence (scaled by marginal variance) between the responses and the predictors which coincides with the chain graphical model [3, 26, 15].

Biologically, conditional regression coefficients are more interpretable than marginal regression coefficients (e.g. the effect of penicillin effect on Gram positive microbes). In particular, given prior knowledge on the behavior of microbes (e.g. laboratory controlled experiments), it is crucial for the regression coefficients to encode *conditional* dependence between nodes and predictors or the biological prior knowledge would be misused.

Despite its biological interpretability, there are downsides to a conditional construction. For example, with conditional coefficients is not possible to do marginal predictions of nodes given that the marginal distribution depends on the regression coefficients of other nodes as well as on the covariance matrix.

In general, it is not possible to perform marginal prediction of single node and graphical selection simultaneously. That is, for $\tilde{\mathbf{B}} = \mathbf{B}\mathbf{\Omega}^{-1}$, marginal prediction requires that $\tilde{\mathbf{B}}$ encodes *marginal* dependence to predictors so that we can take a certain column and use it like the regression coefficient of that single node. On the contrary, graphical selection requires that \mathbf{B} encodes *conditional* dependence. Simultaneous marginal prediction and graphical selection is only possible when $\mathbf{\Omega}^{-1}$ is diagonal, i.e. when nodes are independent, and thus, $\mathbf{B}_{ij} = 0$ implies $\tilde{\mathbf{B}}_{ij} = 0$ for any \mathbf{B} .

Our model focuses on graphical selection, yet we also implement a model for sparse marginal regression coefficient and sparse precision matrix by joining Gibbs sampling for precision matrix in [36] into the Gibbs sampler in [32]. We denote this model Simultaneous Regression and Graphical LASSO (SRG-LASSO) and we use it to compare to the CAR-LASSO in the simulation study (Section 2.5).

2.3 Estimation

2.3.1 Sampling scheme

We can derive an efficient Gibbs sampler for all parameters in this model due to the scale mixture representation. As in [36], let $\mathbf{1}_n$ be the column vector of ones with dimension n , let $\mathbf{S} = \mathbf{Y}^T \mathbf{Y} \in \mathbb{R}^{k \times k}$ (here we have sample as **row** vectors in \mathbf{Y}), let $\hat{\mu} = \mathbf{X}\mathbf{B} + \mathbf{1}_n \mu^T$, and let $\mathbf{U} = \hat{\mu}^T \hat{\mu} \in \mathbb{R}^{k \times k}$. Eq. 3 shows the full conditional distribution of $\mathbf{\Omega}$ and η (the hyperparameters in Eq. 2).

$$p(\mathbf{\Omega}, \eta | \mathbf{Y}, \lambda_{\Omega}, \hat{\mu}) \propto |\mathbf{\Omega}|^{\frac{n}{2}} \exp\left(-\frac{1}{2} \text{tr}(\mathbf{S}\mathbf{\Omega}) - \frac{1}{2} \text{tr}(\mathbf{U}\mathbf{\Omega}^{-1})\right) \prod_{m < l} \left[\frac{1}{\sqrt{2\pi\eta_{ml}}} \exp\left(-\frac{\omega_{ml}^2}{2\eta_{ml}}\right) \right] \times \prod_{m=1}^k \left[\frac{\lambda_{\Omega}}{2} \exp\left(-\frac{\lambda_{\Omega}\omega_{mm}}{2}\right) \right] I_{\mathbf{\Omega} \in M^+} \quad (3)$$

As in [36], we can update one row (column) at one iteration. Let \mathbf{H} be the symmetric matrix with $\mathbf{H}_{ml} = \mathbf{H}_{lm} = \eta_{ml}$ ($m < l$) on the off-diagonal entries and on the diagonal $\mathbf{H}_{mm} = 0$. We take one column out and partition $\mathbf{\Omega}$, \mathbf{S} , \mathbf{U} , and \mathbf{H} . Without loss of generality, we show the sampling scheme for the last row (column). Let $\mathbf{\Omega}_{11} \in \mathbb{R}^{(k-1) \times (k-1)}$, $\omega_{12} \in \mathbb{R}^{k-1}$, and $\omega_{22} \in \mathbb{R}$. We partition \mathbf{S} , \mathbf{U} and \mathbf{H} in the same manner.

$$\mathbf{\Omega} = \begin{bmatrix} \mathbf{\Omega}_{11} & \omega_{12} \\ \omega_{12}^T & \omega_{22} \end{bmatrix}, \mathbf{S} = \begin{bmatrix} \mathbf{S}_{11} & \mathbf{s}_{12} \\ \mathbf{s}_{12}^T & s_{22} \end{bmatrix}, \mathbf{U} = \begin{bmatrix} \mathbf{U}_{11} & \mathbf{u}_{12} \\ \mathbf{u}_{12}^T & u_{22} \end{bmatrix}, \mathbf{H} = \begin{bmatrix} \mathbf{H}_{11} & \eta_{12} \\ \eta_{12}^T & 0 \end{bmatrix}.$$

By setting $\gamma = \omega_{22} - \omega_{12}^T \mathbf{\Omega}_{11}^{-1} \omega_{12} \in \mathbb{R}$, $\mathbf{\Omega}^{-1}$ can be written in a block form [40]:

$$\mathbf{\Omega}^{-1} = \begin{bmatrix} \mathbf{\Omega}_{11}^{-1} + \frac{1}{\gamma} \mathbf{\Omega}_{11}^{-1} \omega_{12} \omega_{12}^T \mathbf{\Omega}_{11}^{-1} & -\frac{1}{\gamma} \mathbf{\Omega}_{11}^{-1} \omega_{12} \\ -\frac{1}{\gamma} \omega_{12}^T \mathbf{\Omega}_{11}^{-1} & \frac{1}{\gamma} \end{bmatrix}.$$

Given

$$\text{tr}(\mathbf{U}\mathbf{\Omega}^{-1}) = \text{tr}(\mathbf{U}_{11}\mathbf{\Omega}_{11}^{-1}) + \frac{1}{\gamma} (\omega_{12}^T \mathbf{\Omega}_{11}^{-1} \mathbf{U}_{11} \mathbf{\Omega}_{11}^{-1} \omega_{12} - 2\mathbf{u}_{12}^T \mathbf{\Omega}_{11}^{-1} \omega_{12} + u_{22}),$$

we have the full conditional distribution of ω_{12} and γ :

$$\begin{aligned}
p(\boldsymbol{\omega}_{12}, \gamma | \boldsymbol{\Omega}_{11}, \eta, \lambda_{\Omega}) &\propto \gamma^{\frac{n}{2}} \exp \left(-\frac{1}{2}(s_{22} + \lambda_{\Omega})\gamma - \frac{u_{22}}{2\gamma} \right) \\
&\times \exp \left\{ -[\mathbf{s}_{12} - \frac{1}{\gamma} \boldsymbol{\Omega}_{11}^{-1} \mathbf{u}_{12}]^T \boldsymbol{\omega}_{12} \right. \\
&\left. - \frac{1}{2} \boldsymbol{\omega}_{12}^T [D_{\eta}^{-1} + (s_{22} + \lambda_{\Omega}) \boldsymbol{\Omega}_{11}^{-1} + \frac{1}{\gamma} \boldsymbol{\Omega}_{11}^{-1} \mathbf{U}_{11} \boldsymbol{\Omega}_{11}^{-1}] \boldsymbol{\omega}_{12} \right\}.
\end{aligned}$$

From the above equation, we get a closed form expression for the conditional distribution of γ :

$$\begin{aligned}
p(\gamma | \boldsymbol{\omega}_{12}, \boldsymbol{\Omega}_{11}, \eta, \lambda_{\Omega}) &\propto \\
\gamma^{\frac{n}{2}} \exp \left(-\frac{1}{2}(s_{22} + \lambda_{\Omega})\gamma - \frac{u_{22} - 2\mathbf{u}_{12}^T \boldsymbol{\Omega}_{11}^{-1} \boldsymbol{\omega}_{12} + \boldsymbol{\omega}_{12}^T \boldsymbol{\Omega}_{11}^{-1} \mathbf{U}_{11} \boldsymbol{\Omega}_{11}^{-1} \boldsymbol{\omega}_{12}}{2\gamma} \right) &I_{\gamma \geq 0}
\end{aligned} \tag{4}$$

which is a Generalized Inverse Gaussian (GIG) distribution [18, 20] with parameters:

$$\begin{aligned}
\lambda &= \frac{n}{2} + 1 \\
\psi &= s_{22} + \lambda_{\Omega} \\
\chi &= u_{22} - 2\mathbf{u}_{12}^T \boldsymbol{\Omega}_{11}^{-1} \boldsymbol{\omega}_{12} + \boldsymbol{\omega}_{12}^T \boldsymbol{\Omega}_{11}^{-1} \mathbf{U}_{11} \boldsymbol{\Omega}_{11}^{-1} \boldsymbol{\omega}_{12}.
\end{aligned}$$

GIG has a positive support. Thus, the determinant and the k^{th} principle minor of the updated $\boldsymbol{\Omega}$ are positive, while the first $k - 1$ principle minors remain unchanged and positive. In this manner, the updated $\boldsymbol{\Omega}$ always remains positive definite.

By denoting $\mathbf{D}_{\eta} = \text{diag}(\boldsymbol{\eta}_{12}) \in \mathbb{R}^{(k-1) \times (k-1)}$, the full conditional distribution of $\boldsymbol{\omega}_{12}$ is a Normal distribution:

$$\begin{aligned}
p(\boldsymbol{\omega}_{12} | \gamma, \boldsymbol{\Omega}_{11}, \eta, \lambda_{\Omega}) &\propto \exp \left\{ -[\mathbf{s}_{12} - \frac{1}{\gamma} \boldsymbol{\Omega}_{11}^{-1} \mathbf{u}_{12}]^T \boldsymbol{\omega}_{12} \right. \\
&\left. - \frac{1}{2} \boldsymbol{\omega}_{12}^T [\mathbf{D}_{\eta}^{-1} + (s_{22} + \lambda_{\Omega}) \boldsymbol{\Omega}_{11}^{-1} + \frac{1}{\gamma} \boldsymbol{\Omega}_{11}^{-1} \mathbf{U}_{11} \boldsymbol{\Omega}_{11}^{-1}] \boldsymbol{\omega}_{12} \right\}
\end{aligned} \tag{5}$$

with parameters:

$$\begin{aligned}
\boldsymbol{\Sigma}_{\boldsymbol{\omega}_{12}}^{-1} &= \mathbf{D}_{\eta}^{-1} + (s_{22} + \lambda_{\Omega}) \boldsymbol{\Omega}_{11}^{-1} + \frac{1}{\gamma} \boldsymbol{\Omega}_{11}^{-1} \mathbf{U}_{11} \boldsymbol{\Omega}_{11}^{-1} \\
\boldsymbol{\mu}_{\boldsymbol{\omega}_{12}} &= -\boldsymbol{\Sigma}_{\boldsymbol{\omega}_{12}} [\mathbf{s}_{12} - \frac{1}{\gamma} \boldsymbol{\Omega}_{11}^{-1} \mathbf{u}_{12}].
\end{aligned}$$

As in [36], the $z_{ij} = 1/\eta_{ij}$ are independent inverse Gaussians with parameters:

$$\begin{aligned}
\mu_{z_{ij}} &= \sqrt{\lambda_{\Omega}^2 / \omega_{ij}^2} \\
\lambda_{z_{ij}} &= \lambda_{\Omega}^2
\end{aligned}$$

and density:

$$p(z_{ij} | \boldsymbol{\Omega}, \lambda_{\Omega}) = \left(\frac{\lambda_{z_{ij}}}{2\pi z_{ij}^3} \right)^{1/2} \exp \left(\frac{-\lambda_{z_{ij}} (z_{ij} - \mu_{z_{ij}})^2}{2(\mu_{z_{ij}})^2 z_{ij}} \right) I_{z_{ij} > 0}.$$

The full conditional distribution of $\text{vec}(\mathbf{B})$ can be represented using tensor product [27]. Let $\mathbf{D}_{\tau^2} = \text{diag}(\tau^2) \in \mathbb{R}^{kp \times kp}$ for τ the scaling parameters in the prior density of \mathbf{B} (Eq. 2). Then, the conditional distribution of $\text{vec}(\mathbf{B})$ has the following form:

$$\begin{aligned}
p(\text{vec}(\mathbf{B}) | \mathbf{D}_{\tau^2}, \boldsymbol{\Omega}, \boldsymbol{\mu}, \mathbf{X}, \mathbf{Y}) &\propto \exp \{ \mathbf{X}^T (\mathbf{Y} - \mathbf{1}_n \boldsymbol{\mu}^T \boldsymbol{\Omega}^{-1}) \\
&- \frac{1}{2} \text{vec}(\mathbf{B})^T (\boldsymbol{\Omega}^{-1} \otimes \mathbf{X}^T \mathbf{X} + \mathbf{D}_{\tau^2}^{-1}) \text{vec}(\mathbf{B}) \}.
\end{aligned} \tag{6}$$

Note that the information from data is encoded by $\boldsymbol{\Omega}^{-1} \otimes \mathbf{X}^T \mathbf{X}$ which differs from the canonical parameterization of the multiresponse linear regression model in which the information from data is encoded by $\boldsymbol{\Omega} \otimes \mathbf{X}^T \mathbf{X}$. This is

because in the kernel of the likelihood, the term involving \mathbf{B} is $\mathbf{X}_i \mathbf{B} \Omega^{-1} \Omega \Omega^{-1} \mathbf{B}^T \mathbf{X}_i^T = \mathbf{X}_i \mathbf{B} \Omega^{-1} \mathbf{B}^T \mathbf{X}_i^T$, instead of $\mathbf{X}_i \tilde{\mathbf{B}} \Omega \tilde{\mathbf{B}}^T \mathbf{X}_i^T$ as in the canonical parametrization (see Section 2.2).

Finally, we update τ_{ij}^2 using an Inverse Gaussian distribution with parameters $\sqrt{\lambda_\beta^2 / \mathbf{B}_{ij}^2}$ and λ_β^2 , and we update μ using a Normal distribution with mean $(\mathbf{Y} \Omega - \mathbf{X} \mathbf{B})^T$ and variance Ω/n .

2.3.2 Choice of hyperparameters

The shrinkage parameters λ_Ω and λ_β (Eq. 2) are hyperparameters to be determined. As in [32, 36], we assume these shrinkage parameters have a hyperprior Gamma distribution with shape parameter r and rate parameter δ which can be set to produce a relatively flat density for a non-informative prior scenario. Note that since the prior on Ω is not a Laplacian but a graphical LASSO prior [36], the Gamma prior is on λ , not on λ^2 as it would be under a LASSO prior.

$$\lambda_\beta^2 \sim \text{Gamma}(r_\beta, \delta_\beta)$$

$$\lambda_\Omega \sim \text{Gamma}(r_\Omega, \delta_\Omega)$$

The shrinkage parameters λ_Ω and λ_β are included in the Gibbs sampler with full conditional distribution still Gamma with shape parameters $r_\beta + kp, \delta_\beta + \sum \tau_i/2$ and rate parameters $r_\Omega + k(k+1)/2, \delta_\Omega + \|\Omega\|_1/2$ respectively.

2.3.3 Graphical structure learning

Our model has a zero posterior probability for a parameter to be zero given the continuous priors. Yet, we still need to determine the cases when the edges of the graph will be considered "non-existent". Here, we infer the graph structure using the horseshoe method in [7, 36] which compares the LASSO estimate for the regression coefficient with the posterior mean of a standard conjugate (non-shrinkage) prior [19].

Let $\pi = \frac{\tilde{\theta}}{E_g(\tilde{\theta}|\mathbf{Y})}$ where $\tilde{\theta}$ represents the estimate of the parameter under the LASSO prior and $E_g(\tilde{\theta}|\mathbf{Y})$ is the posterior mean of that parameter under non-shrinkage prior (e.g. Normal for \mathbf{B} and Washart for Ω). The statistics $1 - \pi$ characterizes the amount of shrinkage due to the LASSO prior. We use $\pi > 0.5$ as the threshold to decide that $\theta \neq 0$ as in [36].

2.4 Extensions

2.4.1 Adaptive LASSO

One simple extension to LASSO was Adaptive LASSO, in which the shrinkage parameter λ can be different for all elements in \mathbf{B} and Ω [27, 36]. This extension is particularly useful when we have prior knowledge of independence among certain nodes.

As suggested in [27, 36], we set the hyperpriors on $\lambda_{ij,\beta}^2$ as Gamma distributions with shape parameters $r_{ij,\beta}$ and rate parameter $\delta_{\beta,ij}$. We also set the prior suggested in [36] for $\lambda_{ij,\Omega}$ (with $i \neq j$). While in [36] shrinkage on diagonal $\lambda_{ii,\Omega}$ is a hyperparameter, we set it here to 0. That is, we are not shrinking the diagonal entries of Ω . But such shrinkage can be included (if so, multiply $\prod_{i=1}^k \frac{\lambda_{ii}}{2} \exp(-\lambda_{ii,\Omega} \omega_{ii})$ to the prior of Ω).

The prior for Ω is

$$p(\Omega | \{\lambda_{ij,\Omega}\}_{i < j}) = C_{\{\lambda_{ij,\Omega}\}_{i < j}}^{-1} \prod_{i < j} \frac{\lambda_{ij,\Omega}}{2} \exp(-\lambda_{ij,\Omega} |\omega_{ij}|) I_{\Omega \in M_+}$$

$$p(\{\lambda_{ij,\Omega}\}_{i < j}) \propto C_{\{\lambda_{ij,\Omega}\}_{i < j}} \prod_{i < j} \frac{1}{\Gamma(r_{ij,\Omega})} \lambda_{ij,\Omega}^{r_{ij,\Omega}-1} \exp(-\delta_{ij,\Omega} \lambda_{ij,\Omega}).$$

The full conditional distribution of the shrinkage parameters is then Gamma (shape and rate parametrization):

$$\lambda_{ij,\Omega} | \Omega \sim \text{Gamma}(r_{ij,\Omega} + 1, \delta_{ij,\Omega} + |\omega_{ij}|), i \neq j$$

$$\lambda_{ij,\beta}^2 | \tau \sim \text{Gamma}(r_{ij,\beta} + 1, \delta_{ij,\beta} + \tau_{ij}/2).$$

We set the hyperparameters as $r = 10^{-2}$ and $\delta = 10^{-6}$ for both Ω and \mathbf{B} [36, 27] with a small value of δ selected to take advantage of the adaptiveness of the shrinkage.

2.4.2 Other types of responses

The model has been defined for continuous responses, yet there are different extensions for the case of binary data, counts and compositional data that we describe below.

Probit model for binary data. For binary responses, we can use a Probit model with CAR in the core of the dependence structure. We denote the CAR latent variable as $\mathbf{Z}_i \in \mathbb{R}^k$, and let $\Phi(Z_{ij})$ model the probability of observing a 1 where Φ is the cumulative distribution function of a standard Normal.

Eq. 7 shows the alternative representation of the model:

$$\begin{aligned} \mathbf{Z}_i &\sim N(\Omega^{-1}(\mathbf{B}^T \mathbf{X}_i^T + \mu), \Omega^{-1}) \\ Y_{ij}^* &\sim N(Z_{ij}, 1) \\ Y_{ij} &= \mathbf{1}_{Y_{ij}^* > 0} \end{aligned} \quad (7)$$

Then, the full conditional probability of Y_{ij}^* is a truncated Normal with mean Z_{ij} and variance 1. By denoting $\hat{\mu}_i = (\mathbf{B}^T \mathbf{X}_i^T + \mu)$, we have the full conditional distribution of \mathbf{Z}_i :

$$\mathbf{Z}_i | Y_i^*, \hat{\mu}_i, \Omega \sim N([\Omega + I]^{-1}(\hat{\mu}_i + Y_i^*), [\Omega + I]^{-1}).$$

Log-normal Poisson model for counts. To model a response of multivariate counts, we use a Lognormal-Poisson model [1]. Let $\mathbf{Z}_i \in \mathbb{R}^k$ be the latent vector of log expected counts of the i^{th} sample and let $\mathbf{Y}_i \in \mathbb{N}^k$ be the observed counts. We use $\mathbf{Z}_{i,-j} \in \mathbb{R}^{k-1}$ to denote the vector of log expected counts of the i^{th} sample but without response j and Z_{ij} as the log expected counts of the i^{th} sample and j^{th} response.

The covariance matrix accounts for both over-dispersion and correlation of the counts:

$$\begin{aligned} \mathbf{Z}_i &\sim N(\Omega^{-1}(\mathbf{B}^T \mathbf{X}_i^T + \mu), \Omega^{-1}) \\ \lambda_{ij} &= \exp(Z_{ij}) \\ Y_{ij} &\sim \text{Poisson}(\lambda_{ij}). \end{aligned} \quad (8)$$

Then, the density of Y_{ij} is:

$$p(Y_{ij} | Z_{ij}) \propto \exp\{Y_{ij} Z_{ij} - e^{Z_{ij}}\}.$$

Let $Z_{ij} | \mathbf{Z}_{i,-j} \sim N(\tilde{\mu}_{ij}, \tilde{\sigma}_{ij}^2)$ be the conditional prior so that the log full conditional is:

$$\log[p(Z_{ij} | \mathbf{Z}_{i,-j}, \hat{\mu}, \Omega, Y)] = Y_{ij} Z_{ij} - \exp(Z_{ij}) - \frac{1}{2\tilde{\sigma}_{ij}^2} (Z_{ij} - \tilde{\mu}_{ij})^2 + C$$

which is clearly concave.

This means that we can sample the full conditional distribution of the latent variables using adaptive rejection sampling (ARS) [16], and this can be done in parallel to further speed up the sampling.

Normal-Logistic for multinomial data. As in [39], we developed a Normal-Logistic model for multinomial compositional data. This type of data is very common in microbiome and ecology studies.

Assume that we have $k + 1$ responses in our sample and the last response serves as reference group. Let $\mathbf{Z}_i \in \mathbb{R}^{k+1}$ denote the latent vector of logit transformed relative abundance for i th sample, and let $\mathbf{Y}_i \in \mathbb{N}^k$ be the observed species counts. Denote as M the known total count (e.g. sequence depth in microbiome studies). Similarly we use $\mathbf{Z}_{i,-j}$ to denote the vector logit transformed relative abundance of the i th sample but without response j and Z_{ij} as the log expected counts of the i th sample and j th response.

The Normal-Logistic model has the following structure:

$$\begin{aligned} \mathbf{Z}_i &\sim N(\Omega^{-1}(\mathbf{B}^T \mathbf{X}_i^T + \mu), \Omega^{-1}) \\ p_{ij} &= \frac{\exp(Z_{ij})}{\sum_{i=1}^k \exp(Z_{ij}) + 1} \\ \mathbf{Y}_i &\sim \text{Multinomial}(p_{i1}, \dots, p_{ik}, M) \end{aligned} \quad (9)$$

Note that the normal latent variables take care of the over-dispersion, so a key part of the model is the sampling the latent variable.

Then, the likelihood of \mathbf{Y}_i is:

$$p(\mathbf{Y}_i|\mathbf{Z}_i) = \frac{1}{\sum_{j=1}^k \exp(Z_{ij}) + 1} \prod_{j=1}^k \frac{\exp(Y_{ij}Z_{ij})}{\sum_{j=1}^k \exp(Z_{ij}) + 1}$$

Let $Z_{ij}|\mathbf{Z}_{i,-j} \sim N(\tilde{\mu}_{ij}, \tilde{\sigma}_{ij}^2)$ be the conditional prior so that the log full conditional is:

$$\log[p(Z_{ij}|\mathbf{Z}_{i,-j}, \tilde{\mu}, \Omega, Y)] = Y_{ij}Z_{ij} - N \log \left(\sum_{j=1}^k \exp(Z_{ij}) + 1 \right) - \frac{1}{2\tilde{\sigma}_{ij}^2} (Z_{ij} - \tilde{\mu}_{ij})^2 + C$$

This function is concave because the first term is an affine, the second term is the negative log sum of exponential of an affine function, and the last term is a concave quadratic form. Thus, ARS [16] can again be used during the Gibbs sampling, and this process can be parallelized for extra speed.

2.5 Simulations

We simulate data under the six graphical structures in [36] with $k = 30, n = 50$. We vary the sparsity of \mathbf{B} with 80% or 50% entries equal to zero (denoted beta sparsity of 0.8 and 0.5 in the figures) and a grand mean (i.e. intercept μ) of 0. Each simulation setting was repeated 50 times.

The six graphical structures are defined below. Note that model 1 and model 3 specify the entries of the covariance matrix Σ (σ_{ij}) while the other models specify the entries of the precision matrix Ω (ω_{ij}).

- Model 1: An AR(1) model with $\sigma_{ij} = 0.7^{|i-j|}$
- Model 2: An AR(2) model with $\omega_{ii} = 1, \omega_{i-1,i} = \omega_{i,i-1} = 0.5, \omega_{i-2,i} = \omega_{i,i-2} = 0.25$ for $i = 1, \dots, k$
- Model 3: A block model with $\sigma_{ii} = 1$ for $i = 1, \dots, k, \sigma_{ij} = 0.5$ for $1 \leq i \neq j \leq k/2, \sigma_{ij} = 0.5$ for $k/2 + 1 \leq i \neq j \leq 10$ and $\sigma_{ij=0}$ otherwise.
- Model 4: A star model with every node connected to the first node, with $\omega_{ii} = 1, \omega_{1,i} = \omega_{i,1} = 0.1$ for $i = 1, \dots, k$, and $\omega_{ij} = 0$ otherwise.
- Model 5: A circle model with $\omega_{ii} = 2, \omega_{i-1,i} = \omega_{i,i-1} = 1$ for $i = 1, \dots, k$, and $\omega_{1,k} = \omega_{k,1} = 0.9$ for $j = 1, \dots, k$.
- Model 6: A full model with $\omega_{ii} = 2$ and $\omega_{ij} = 1$ for $i \neq j \in \{1, \dots, k\}$.

We compare the performance of 8 methods:

1. CAR-LASSO: our proposed model
2. Adaptive CAR-LASSO: our proposed model with different shrinkage parameters for \mathbf{B} and Ω
3. SRG-LASSO: our model focused on marginal prediction described in Section 2.2
4. Graphical LASSO in [36]
5. Adaptive Graphical LASSO: adaptive version in [36]
6. Multivariate regression: Bayesian multi-response regression with conjugate priors. Since this model does not really estimate the conditional regression coefficients \mathbf{B} but the marginal regression coefficient $\tilde{\mathbf{B}}$, we get $\mathbf{B} = \tilde{\mathbf{B}}\Omega$ (see Section 2.2)
7. Multivariate regression with 0 mean: Bayesian multi-response regression with conjugate priors that assume the marginal mean is 0 (similar to Graphical LASSO)
8. Calculate the empirical covariance matrix and take inverse (denoted ad-hoc in the figures)

As in [36, 27], we set the hyperparameters of the Gamma hyperprior for the shrinkage parameters of both \mathbf{B} and Ω as $r = 0.01, \delta = 10^{-6}$ for the adaptive versions, and $r = 1, \delta = 0.01$ for the non-adaptive versions.

To evaluate the performance of the methods, we compute the L2-loss of the estimate of \mathbf{B} and the Stein's loss of the estimate of Ω . To our knowledge, there is no convention for which loss should be used. We use Stein's loss for Ω since it is the KL-divergence when the mean vector is 0.

In addition, we evaluate the reconstruction of the graphical structures based on the Matthews Correlation Coefficient (MCC) [12] which range from -1 to 1 with 1 representing a perfect prediction. Given that the covariance model 6 is a fully connected graph (and thus, there are no true negatives or false positives), we did not calculate the MCC in this case. In multivariate regression, we consider any edge with weight $< 1 \times 10^{-3}$ to be 0.

2.6 Real Data

We test our method on two microbial compositional datasets:

- **Soil microbiota data.** The objective of this study [17, 5] is to examine soil microbial community composition and structure of both bacteria and fungi at a microbially-relevant scale. The researchers isolated soil aggregates from three land management systems in central Iowa to test if the aggregate-level microbial responses are related to plant community and management practices. The clean dataset has 120 samples with 17 genus under consideration. We focus on the bacteria to further evaluate the partial association among them and the environmental factors.
- **Human gut microbiota data.** The microbiota of older people displays greater inter-individual variation than that of younger adults. This study [10, 31] collected faecal microbiota composition from 178 elderly subjects, together with subjects' residence type (in the community, day-hospital, rehabilitation or in long-term residential care) and diet. Researchers studied the correlation between microbes and other measurements. We evaluate the partial correlation between environments and among microbes in those elderly subjects.

We use the MG-RAST server [30] for profiling with an e-value of 5, 60% identity, alignment length of 15 bp, and minimal abundance of 10 reads. Unclassified hits are not included in the analysis. Genus with more than 0.5% (human) or 1% (soil) relative abundance in more than 50 samples is selected as the focal genus and all other genus serve as the reference group.

We reconstruct the weighted graph using the conditional regression coefficient between any two nodes. The α -centrality [6] is used to identify the importance of nodes. Weighted adjacency matrix is constructed with the posterior mean of the conditional regression coefficients of those that showed significance with the horseshoe method described in Section 2.3.3.

3 Results

3.1 Computational Speed and Scaling

We test the scalability of our estimation procedure by simulating 500 and 1000 samples with 5, 10, 25, 50, 100 nodes. We sample 1000 generations with 100 burn-in on a machine with Core-i7 4790 CPU and Windows 7 operating system. We record CPU seconds in R.

While our models are slower than Graphical LASSO or multivariate regression, running time is not severely impacted by sample size (Fig. 2). Instead, speed is mostly influenced by the number of nodes and the number of predictors. However, even the case of 100 nodes and 10 predictors is successfully completed in less than 10 minutes.

3.2 Simulations

Our proposed models (CAR-LASSO and adaptive CAR-LASSO) outperform the other models in almost every covariance model and sparsity setting with the adaptive version outperforming the non-adaptive version in almost every setting in reconstructing the precision matrix evaluated by Stein's loss (Fig. 3)

Similarly, our proposed models (CAR-LASSO and adaptive CAR-LASSO) outperform the other models in almost every covariance model and sparsity setting in reconstructing the regression coefficient matrix evaluated by L2 loss (Fig. 4). However, unlike in the case of Ω , the adaptive version did not outperform the non-adaptive version in some scenarios especially when B is not sparse.

Graphical LASSO and Adaptive Graphical LASSO are not included in this plot because these models do not estimate the matrix of regression coefficients B .

In all cases, adaptive CAR-LASSO had highest MCC in both precision and regression coefficients (Fig. 5 for precision matrix and 6 for regression coefficients). There is one exception of covariance model 4 where all models performed poorly. This might due to the difficulty of finding the center of the graph in this model.

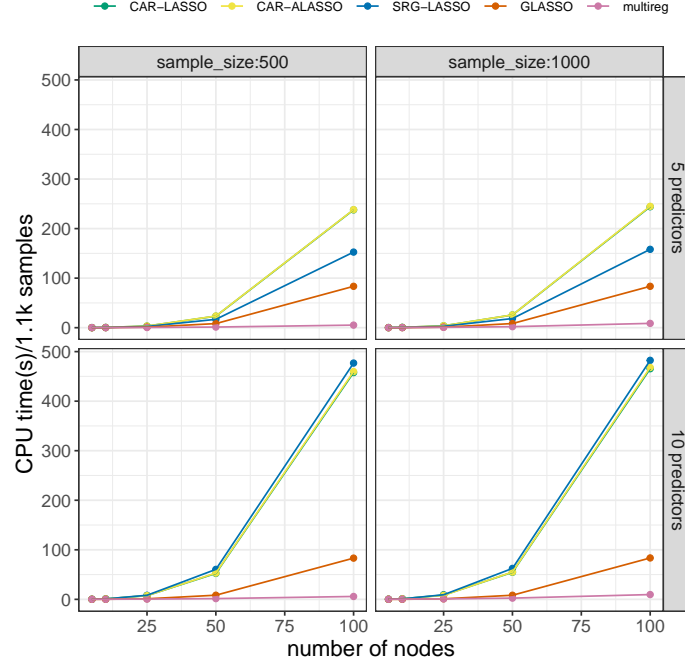


Figure 2: **Scalability test.** Computational time for each algorithm in CPU seconds as a function of the number of nodes, the number of predictors, and sample size. Speed depends on the number of nodes and number of predictors, but not on sample size. Our proposed method is efficient, yet slower than Graphical LASSO

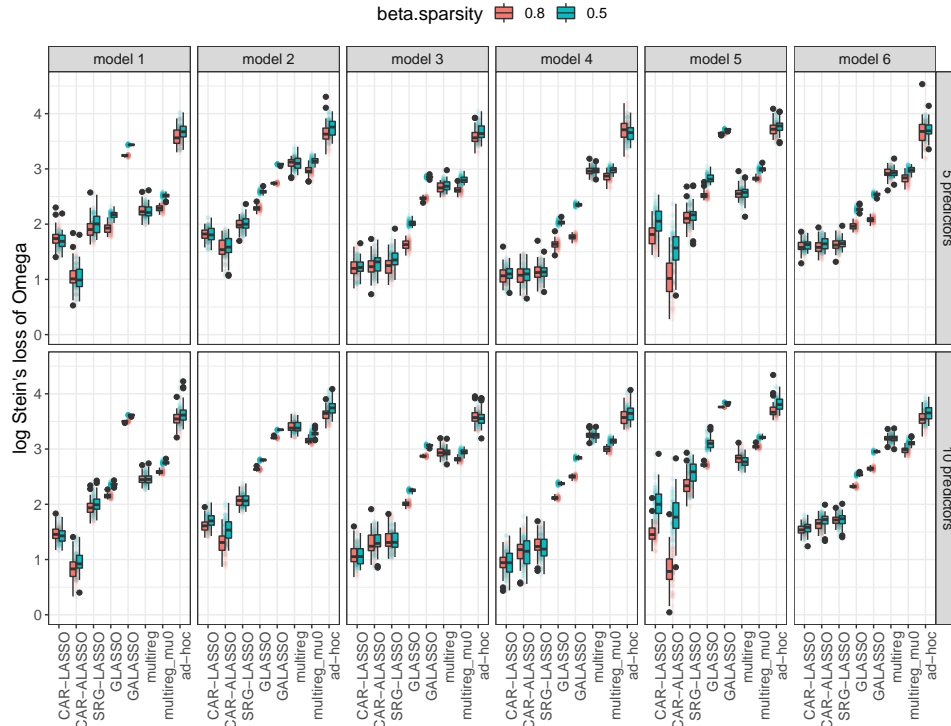


Figure 3: **Stein's Loss of Ω ,** (Y-axis in logarithmic scale) for simulated datasets with 30 nodes and 50 samples under two levels of beta sparsity (red 0.8 and blue 0.5), two different number of predictors (10 in bottom row and 5 in top row) and six covariance models (columns). X-axis corresponds to the models compared. Our models (Adaptive) CAR-LASSO get the lowest loss in most cases.

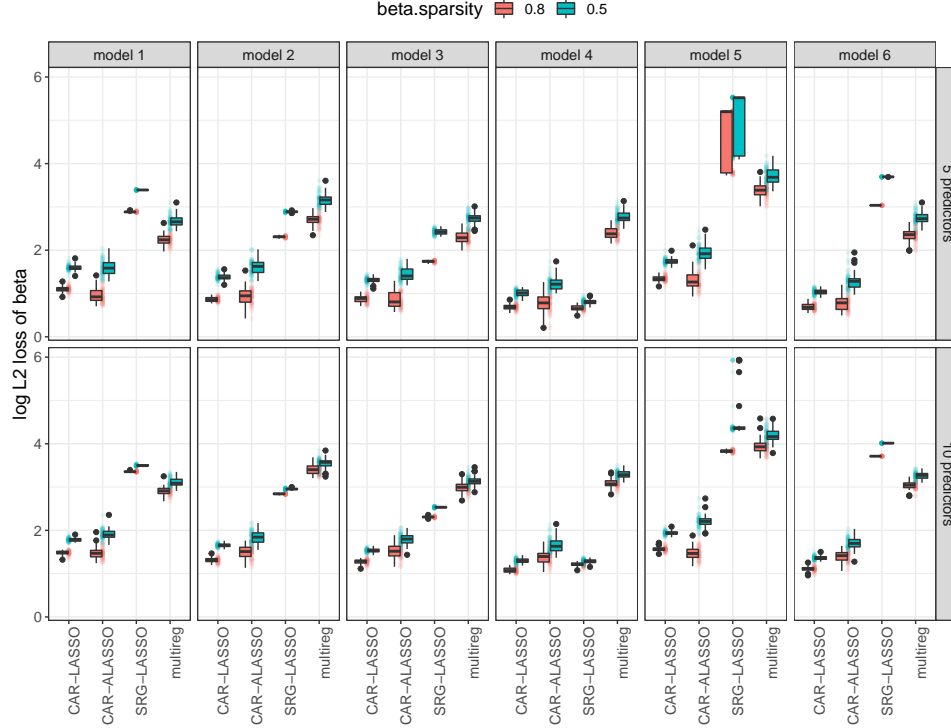


Figure 4: **L2 Loss of β** (Y-axis in logarithmic scale) for simulated datasets with 30 nodes and 50 samples under two levels of beta sparsity (red 0.8 and blue 0.5), two different number of predictors (10 in bottom row and 5 in top row) and six covariance models (columns). X-axis corresponds to the models compared. Our models (Adaptive) CAR-LASSO get the lowest loss in most cases.

3.3 Soil and Human Gut Microbiome

The soil microbiota (Fig. 8) results in a more dense network compared to the human gut (Fig. 7). In the human gut microbiota network, the edges with the most weight correspond to connections between genus nodes, not so much with predictors. The most important predictor is whether the patient’s residence was a long-term residential care which positively affected genus *Caloramator*. This results agrees with the original analysis that also separates elderly subjects based upon where they live in the community. Another important predictor was Diet Group 4 which corresponds to the high fat/low fiber group. This diet positively affected genus *Caloramator* as well. In the soil microbiota network, the most important link is between *Candidatus Solibacter* and *Candidatus Koribacter*. There are not important connections with predictors in this case. These results agree with the original research that indicated that core microbial communities within soil aggregates are likely driven by stable and long-term factors such as clay content rather than relative short time scaled land management as the ones considered as predictors in this study.

It is worth highlighting that our model can produce meaningful results from relative small sample sizes: 120 samples for the soil microbiota study and 178 samples for the human gut microbiota study.

4 Discussion

Importance of conditional dependence. It is crucial for any model dealing with predictors and multivariate responses to distinguish between marginal effects and conditional effects. A conditional construction coincides with the intuition that the marginal response of a node *should* be influenced by both its and others’ reaction to a common input. This distinction of marginal or conditional effect is particularly important when including biological prior knowledge. For example, species reactions to treatments can be measured under controlled experiments (e.g. [28]) and this knowledge would be properly encoded under a conditional dependence model. See more in the “Agreement with experimenter’s intuition on mean behavior” and “Optimal model-based design of experiments”.

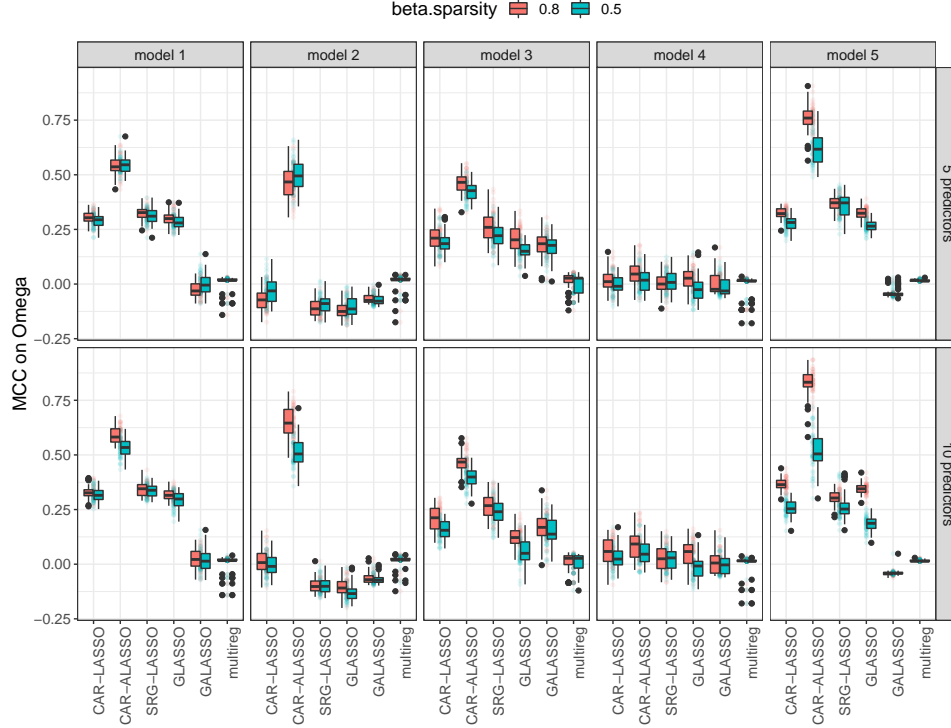


Figure 5: **Matthews Correlation Coefficients for Ω** for simulated datasets with 30 nodes and 50 samples under two levels of beta sparsity (red 0.8 and blue 0.5), two different number of predictors (10 in bottom row and 5 in top row) and six covariance models (columns, fully connected covariance model was omitted from Ω result since MCC was not defined). X-axis corresponds to the models compared. MCC=1 means a perfect reconstruction. Our model Adaptive CAR-LASSO gets the highest MCC in most cases.

Flexibility of the Bayesian model. Compared with the frequentist method, the Bayesian method allows an easier extension of the core Normal model to different types of responses via hierarchical structures. As long as one can sample from the full conditional distribution of the (latent) Normal variable, the posterior sampling is a straight-forward extension of the proposed Gibbs sampler. Though not shown here, other commonly encountered models in biology are also simple extensions of our model, e.g. zero-inflated Poisson and multinomial [22]. By using the Normal distribution as the core model, we can automatically take into account the over-dispersion because the model considers the variance parameters explicitly. In addition, one common complaint on the LASSO prior is that it does not put any mass on 0 for any edge. Though a spike-slab prior is possible, an efficient posterior sampling algorithm like the block Gibbs sampler in [36] and in this work would be hard to derive due the intractable normalizing constant.

Challenges of graph learning. Graphical selection can be difficult because of the confounding in its own structure. For example, recall Fig. 1 A and B. These two graphs can produce a similar correlation between Y_1 and Y_2 . One extreme example is when all links in A and B have no noise (e.g. $Y_1 = X$, $Y_2 = -Y_1$ versus $Y_1 = X$, $Y_2 = -X$). In this extreme example, it is impossible to distinguish graph A from B. Of particular difficulty are also cases like Fig. 1 E where all partial correlations are positive (or negative). Additionally, when Ω has bad condition numbers, then \mathbf{B} might have large error in estimation since the marginal mean response and Ω inform the estimation of \mathbf{B} , and a small change in the marginal mean response can have a large influence in \mathbf{B} .

Agreement with experimenter's intuition on mean behavior. Intuitively, an experimenter should be able to make inferences about the interactions among responses from the behavior of the mean structures under treatment. For example, in Fig. 1 D, an experimenter might knock out a gene as the treatment ($X = 1$ for knock out and $X = 0$ for not) and compare the gene expression levels of another gene (Y_2) via a t test. The result of this t test will provide information regarding the interaction between Y_1 and Y_2 because there are no other factors affecting Y_1 and X is conditionally independent with Y_2 . Thus, this experiment is specific to Y_1 and provides information on partial correlation between Y_1 and Y_2 by only affecting Y_1 . That is, any change in Y_2 is due to the partial correlation with Y_1 rather than a reaction to X . It is precisely the fact that the mean of Y_2 in this experiment depends on the correlation between Y_1 and Y_2

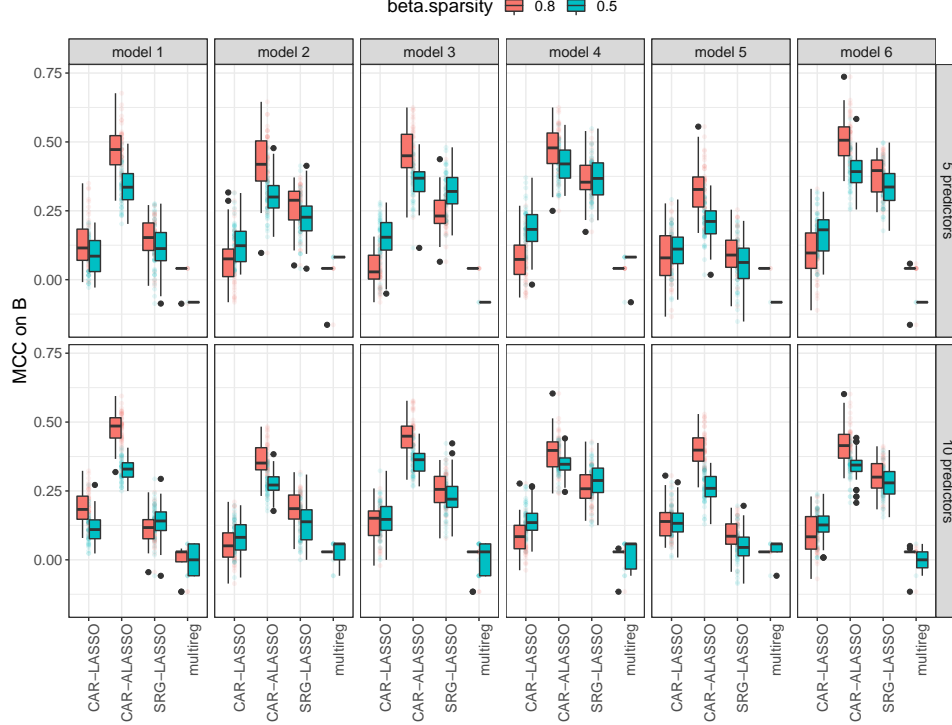


Figure 6: **Matthews Correlation Coefficients for B** for simulated datasets with 30 nodes and 50 samples under two levels of beta sparsity (red 0.8 and blue 0.5), two different number of predictors (10 in bottom row and 5 in top row) and six covariance models (columns, fully connected covariance model was omitted from Ω result since MCC was not defined). X-axis corresponds to the models compared. MCC=1 means a perfect reconstruction. Our model Adaptive CAR-LASSO gets the highest MCC in most cases.

that allows experimenters to test differences in means of Y_2 under the effect of the treatment (X) through standard t tests. However, this intuition is violated though under the standard linear regression setting. The vector (Y_1, Y_2) is Normally distributed with mean $\mu = (X\beta_1, 0)$ and covariance Σ under the network in Fig. 1 D, and thus, the mean of Y_2 is always 0 regardless of the value of X . In contrast, in the CAR parametrization, the mean vector is $\Sigma\mu$ whose second entry is given by $\rho\beta_1X$, i.e. the mean value of Y_2 depends on β_1 (the reaction of Y_1 to the treatment) as well as ρ (the correlation between Y_1 and Y_2). Given that the experimenter’s intuition on specificity is based on the notion of *conditional (in)dependence* between X and Y_1, Y_2 , we conclude that it is desirable that the mean vector contains information on the correlation structure among responses and this is a characteristic of the CAR model that we propose.

Optimal model-based design of experiments. An experimenter should be able to design experiments that decode the links among response nodes when specific experimental interventions towards one node are possible. In practice, when possible, experimenters will always prefer experiments with better specificity. However, this preference is not evident in the linear regression setting since the Fisher information matrix of the mean vector and the precision matrix is block-diagonal [29], and thus, any information that we have on B will not affect estimation of Σ . In addition, the information of Σ is not a function of design (X) no matter whether we have prior knowledge about effect of such experiment (prior on B). Using the CAR parametrization avoids this disagreement because the Fisher information matrix is no longer block-diagonal and prior information about the treatment can flow into the estimation of Σ via an optimal model-based experimental design [9]. We highlight that due to the confounding between the treatment effect and the interaction among responses, the prior knowledge on specificity of the treatment is necessary for such an optimal model-based experimental design.

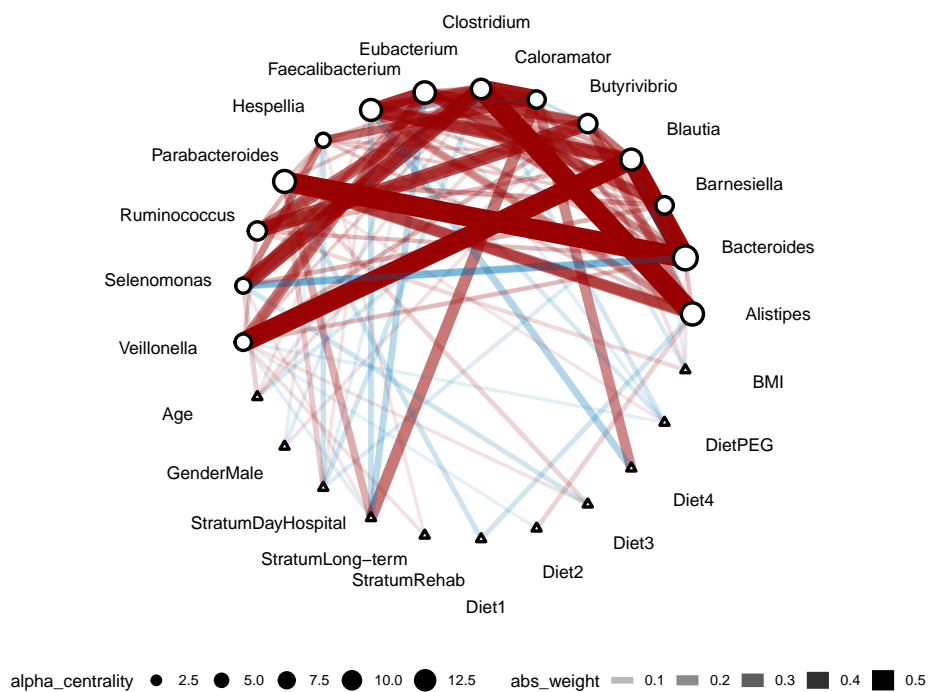


Figure 7: **Reconstructed genus network for human gut microbiota.** Triangle nodes correspond to predictors and circle nodes correspond to relative abundances of genus. The node size on the circle nodes correspond to the α -centrality values [6]. The width of the edges correspond to the absolute weight, and the color to the type of interaction (red positive, blue negative).

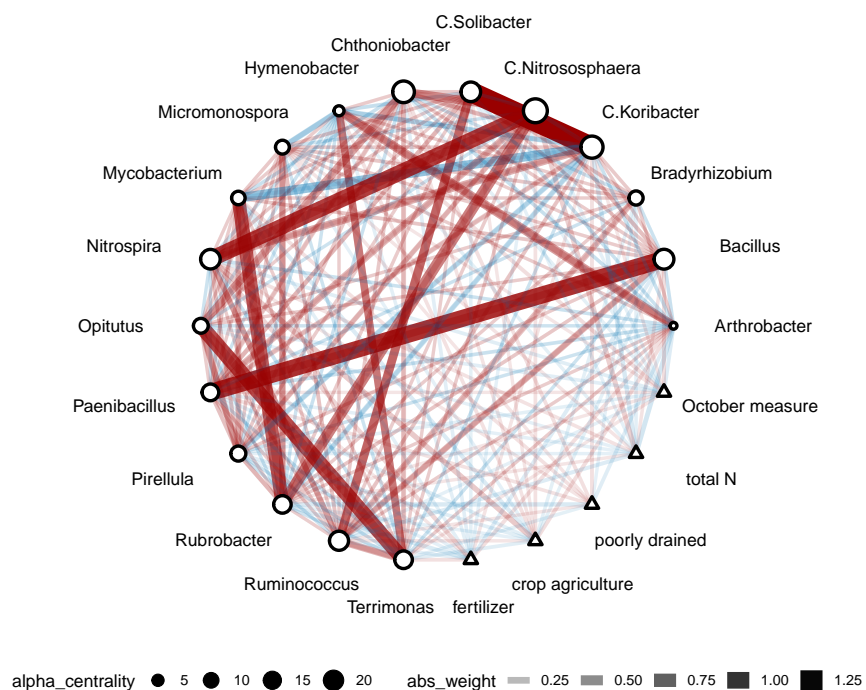


Figure 8: **Reconstructed genus network for soil microbiota.** Triangle nodes correspond to predictors and circle nodes correspond to relative abundances of genus. The node size on the circle nodes correspond to the α -centrality values [6]. The width of the edges correspond to the absolute weight, and the color to the type of interaction (red positive, blue negative).

Acknowledgements

This material is based upon work support by the National Institute of Food and Agriculture, United States Department of Agriculture, Hatch project 1023699. This work was also partially supported by the Department of Energy [DE-SC0021016 to CSL]. Y.S. would like to thank Xiang Li from Peking University for discussion on the Generalized Inverse Gaussian distribution.

References

- [1] J. Aitchison and C. H. Ho. The multivariate Poisson-log normal distribution. *Biometrika*, 76(4):643–653, 12 1989.
- [2] Cassandra Allsup and Richard Lankau. Migration of soil microbes may promote tree seedling tolerance to drying conditions. *Ecology*, 100:e02729, 04 2019.
- [3] Steen A Andersson, David Madigan, and Michael D Perlman. Alternative markov properties for chain graphs. *Scandinavian journal of statistics*, 28(1):33–85, 2001.
- [4] David F Andrews and Colin L Mallows. Scale mixtures of normal distributions. *Journal of the Royal Statistical Society: Series B (Methodological)*, 36(1):99–102, 1974.
- [5] Elizabeth M Bach, Ryan J Williams, Sarah K Hargreaves, Fan Yang, and Kirsten S Hofmockel. Greatest soil microbial diversity found in micro-habitats. *Soil biology and Biochemistry*, 118:217–226, 2018.
- [6] Phillip Bonacich and Paulette Lloyd. Eigenvector-like measures of centrality for asymmetric relations. *Social networks*, 23(3):191–201, 2001.
- [7] Carlos M Carvalho, Nicholas G Polson, and James G Scott. The horseshoe estimator for sparse signals. *Biometrika*, 97(2):465–480, 2010.
- [8] Anna M. Cates, Michael J. Braus, Thea L. Whitman, and Randall D. Jackson. Separate drivers for microbial carbon mineralization and physical protection of carbon. *Soil Biology and Biochemistry*, 133:72–82, 2019.
- [9] Kathryn Chaloner and Isabella Verdinelli. Bayesian experimental design: A review. *Statistical Science*, pages 273–304, 1995.
- [10] Marcus J Claesson, Ian B Jeffery, Susana Conde, Susan E Power, Eibhlís M O’connor, Siobhán Cusack, Hugh MB Harris, Mairead Coakley, Bhuvaneswari Lakshminarayanan, Orla O’Sullivan, et al. Gut microbiota composition correlates with diet and health in the elderly. *Nature*, 488(7410):178–184, 2012.
- [11] Maneesh Dave, Peter D. Higgins, Sumit Middha, and Kevin P. Rioux. The human gut microbiome: current knowledge, challenges, and future directions. *Translational Research*, 160(4):246 – 257, 2012. In-Depth Review: Of Microbes and Men: Challenges of the Human Microbiome.
- [12] Jianqing Fan, Yang Feng, and Yichao Wu. Network exploration via the adaptive lasso and scad penalties. *The annals of applied statistics*, 3(2):521, 2009.
- [13] Noah Fierer, Christian L Lauber, Kelly S Ramirez, Jesse Zaneveld, Mark A Bradford, and Rob Knight. Comparative metagenomic, phylogenetic and physiological analyses of soil microbial communities across nitrogen gradients. *The ISME Journal*, 6(5):1007–1017, 2012.
- [14] Jerome Friedman, Trevor Hastie, and Robert Tibshirani. Sparse inverse covariance estimation with the graphical lasso. *Biostatistics*, 9(3):432–441, 2008.
- [15] Morten Frydenberg. The chain graph markov property. *Scandinavian Journal of Statistics*, pages 333–353, 1990.
- [16] Walter R Gilks and Pascal Wild. Adaptive rejection sampling for gibbs sampling. *Journal of the Royal Statistical Society: Series C (Applied Statistics)*, 41(2):337–348, 1992.
- [17] Kirsten Hofmockel. Hofmockel soil aggregate cob kbase (mgp2592). <https://www.mg-rast.org/mgmain.html?mgpage=project&project=mgp2592>, 2012.
- [18] Wolfgang Hörmann and Josef Leydold. Generating generalized inverse gaussian random variates. *Statistics and Computing*, 24(4):547–557, 2014.
- [19] Beatrix Jones, Carlos Carvalho, Adrian Dobra, Chris Hans, Chris Carter, and Mike West. Experiments in stochastic computation for high-dimensional graphical models. *Statistical Science*, pages 388–400, 2005.
- [20] Bent Jorgensen. *Statistical properties of the generalized inverse Gaussian distribution*, volume 9. Springer Science and Business Media, 2012.

- [21] Christina Kranz and Thea Whitman. Short communication: Surface charring from prescribed burning has minimal effects on soil bacterial community composition two weeks post-fire in jack pine barrens. *Applied Soil Ecology*, 144:134–138, 2019.
- [22] Diane Lambert. Zero-inflated poisson regression, with an application to defects in manufacturing. *Technometrics*, 34(1):1–14, 1992.
- [23] Emily W Lankau, Diane Xue, Rachel Chrisensen, Amanda J Gevens, and Richard A Lankau. Management and soil conditions influence common scab severity on potato tubers via indirect effects on soil microbial communities. *Phytopathology*TM, 2020/02/27 2020.
- [24] Richard Lankau, Isabelle George, and Max Miao. Crop health optimized by microbial diversity across phylogenetic scales. *Submitted*, 2020.
- [25] Steffen L Lauritzen and Thomas S Richardson. Chain graph models and their causal interpretations. *Journal of the Royal Statistical Society: Series B (Statistical Methodology)*, 64(3):321–348, 2002.
- [26] Steffen Lilholt Lauritzen and Nanny Wermuth. Graphical models for associations between variables, some of which are qualitative and some quantitative. *The annals of Statistics*, pages 31–57, 1989.
- [27] Chenlei Leng, Minh Ngoc Tran, and David Nott. Bayesian adaptive Lasso. *Annals of the Institute of Statistical Mathematics*, 66(2):221–244, 2014.
- [28] Chieh Lo and Radu Marculescu. Mplasso: Inferring microbial association networks using prior microbial knowledge. *PLoS computational biology*, 13(12):e1005915, 2017.
- [29] Luigi Malagò and Giovanni Pistone. Information geometry of the gaussian distribution in view of stochastic optimization. In *Proceedings of the 2015 ACM Conference on Foundations of Genetic Algorithms XIII*, pages 150–162, 2015.
- [30] Folker Meyer, Daniel Paarmann, Mark D’Souza, Robert Olson, Elizabeth M Glass, Michael Kubal, Tobias Paczian, Alex Rodriguez, Rick Stevens, Andreas Wilke, et al. The metagenomics rast server—a public resource for the automatic phylogenetic and functional analysis of metagenomes. *BMC bioinformatics*, 9(1):1–8, 2008.
- [31] Paul W O’Toole. Gut microbiota in the irish elderly and its links to health and diet (mgp154). <https://www.mg-rast.org/mgmain.html?mgpage=project&project=mgp154>, 2008.
- [32] Trevor Park and George Casella. The Bayesian Lasso. *Journal of the American Statistical Association*, 103(482):681–686, 2008.
- [33] R. A. Rioux, C. M. Stephens, and J. P. Kerns. Factors affecting pathogenicity of the turfgrass dollar spot pathogen in natural and model hosts. *bioRxiv*, page 630582, 01 2019.
- [34] Peter J Turnbaugh, Ruth E Ley, Micah Hamady, Claire M Fraser-Liggett, Rob Knight, and Jeffrey I Gordon. The human microbiome project. *Nature*, 449(7164):804–810, 2007.
- [35] Jay M. Ver Hoef, Ephraim M. Hanks, and Mevin B. Hooten. On the relationship between conditional (CAR) and simultaneous (SAR) autoregressive models. *Spatial Statistics*, 25:68–85, 2018.
- [36] Hao Wang. Bayesian graphical lasso models and efficient posterior computation. *Bayesian Analysis*, 7(4):867–886, 2012.
- [37] Thea Whitman, Rachel Neurath, Adele Perera, Ilexis Chu-Jacoby, Daliang Ning, Jizhong Zhou, Peter Nico, Jennifer Pett-Ridge, and Mary Firestone. Microbial community assembly differs across minerals in a rhizosphere microcosm. *Environmental Microbiology*, 20(12):4444–4460, 2018.
- [38] Thea Whitman, Ellen Whitman, Jamie Woolet, Mike D. Flannigan, Dan K. Thompson, and Marc-André Parisien. Soil bacterial and fungal response to wildfires in the canadian boreal forest across a burn severity gradient. *Soil Biology and Biochemistry*, 138:107571, 2019.
- [39] Fan Xia, Jun Chen, Wing Kam Fung, and Hongzhe Li. A logistic normal multinomial regression model for microbiome compositional data analysis. *Biometrics*, 69(4):1053–1063, 2013.
- [40] Fuzhen Zhang. *The Schur complement and its applications*, volume 4. Springer Science and Business Media, 2006.